Received: 15 February 2021 | Revised: 11 August 2021 | Accepted: 15 August 2021

DOI: 10.1111/nan.12765

ORIGINAL ARTICLE

Neuropathology and Applied Neurobiology
JOURNAL OF THE BRITISH NEUROPATHOLOGICAL SOCIETY
WILEY

MiR-142-3p regulates synaptopathy-driven disease progression in multiple sclerosis

Francesca De Vito[1] | Alessandra Musella[2,3] | Diego Fresegna[2] | Francesca Romana Rizzo[4] | Antonietta Gentile[2] | Mario Stampanoni Bassi[1] | Luana Gilio[1] | Fabio Buttari[1] | Claudio Procaccini[5,6] | Alessandra Colamatteo[7] | Silvia Bullitta[2,4] | Livia Guadalupi[2,4] | Silvia Caioli[1] | Valentina Vanni[2,4] | Sara Balletta[4] | Krizia Sanna[4] | Antonio Bruno[1,4] | Ettore Dolcetti[1,4] | Roberto Furlan[8] | Annamaria Finardi[8] | Valerio Licursi[9] | Jelena Drulovic[10,11] | Tatjana Pekmezovic[12] | Clorinda Fusco[7] | Sara Bruzzaniti[5,7] | Eran Hornstein[13] | Antonio Uccelli[14,15] | Marco Salvetti[1,16] | Giuseppe Matarese[5,7] | Diego Centonze[1,4] | Georgia Mandolesi[2,3]

[1]Unit of Neurology, IRCCS Neuromed, Pozzilli, Italy

[2]Synaptic Immunopathology Lab, IRCCS San Raffaele Roma, Italy

[3]Department of Human Sciences and Quality of Life Promotion, University of Rome, San Raffaele, Italy

[4]Department of Systems Medicine, Tor Vergata University, Rome, Italy

[5]Laboratorio di Immunologia, Istituto per l'Endocrinologia e l'Oncologia Sperimentale "G. Salvatore", Consiglio Nazionale delle Ricerche, Naples, Italy

[6]Unit of Neuroimmunology, IRCCS—Fondazione Santa Lucia, Rome, Italy

[7]Dipartimento di Medicina Molecolare e Biotecnologie Mediche, Università degli Studi di Napoli "Federico II", Naples, Italy

[8]Neuroimmunology Unit, Institute of Experimental Neurology (INSpe), Division of Neuroscience, San Raffaele Scientific Institute, Milan, Italy

[9]Department of Biology and Biotechnologies "C. Darwin," Laboratory of Functional Genomics and Proteomics of Model Systems, University of Rome "Sapienza", Rome, Italy

[10]Clinic of Neurology, Clinical Center of Serbia, Belgrade, Serbia

[11]Faculty of Medicine, University of Belgrade, Belgrade, Serbia

[12]Faculty of Medicine, Institute of Epidemiology, University of Belgrade, Belgrade, Serbia

[13]Department of Molecular Genetics, Weizmann Institute of Science, Rehovot, Israel

[14]Department of Neurosciences, Rehabilitation, Ophthalmology, Genetics, Maternal and Child Health Unit and Center of Excellence for Biomedical Research, University of Genova, Genoa, Italy

[15]IRCCS Ospedale Policlinico San Martino, Genoa, Italy

[16]Center for Experimental Neurological Therapies, Sant'Andrea Hospital, Department of Neurosciences, Mental Health and Sensory Organs, Sapienza University of Rome, Rome, Italy

Correspondence
Diego Centonze, Department of Systems Medicine, Tor Vergata University, Rome, Italy.
Email: centonze@uniroma2.it

Abstract

Aim: We recently proposed miR-142-3p as a molecular player in inflammatory synaptopathy, a new pathogenic hallmark of multiple sclerosis (MS) and of its mouse model

Francesca De Vito and Alessandra Musella equally contributed to the paper.

Funding information
Fondazione Italiana Sclerosi Multipla; Private donation to DC; Ricerca corrente and '5 per mille' public funding to IRCCS Neuromed; Ricerca corrente to IRCCS San Raffaele Pisana; Italian Ministry of Health; Italian Ministry of University and Research; FISM; Biogen

experimental autoimmune encephalomyelitis (EAE), that leads to neuronal loss independently of demyelination. MiR-142-3p seems to be unique among potential biomarker candidates in MS, since it is an inflammatory miRNA playing a dual role in the immune and central nervous systems. Here, we aimed to verify the impact of miR-142-3p circulating in the cerebrospinal fluid (CSF) of MS patients on clinical parameters, neuronal excitability and its potential interaction with disease modifying therapies (DMTs).

Methods and Results: In a cohort of 151 MS patients, we found positive correlations between CSF miR-142-3p levels and clinical progression, IL-1β signalling as well as synaptic excitability measured by transcranial magnetic stimulation. Furthermore, therapy response of patients with 'low miR-142-3p' to dimethyl fumarate (DMF), an established disease-modifying treatment (DMT), was superior to that of patients with 'high miR-142-3p' levels. Accordingly, the EAE clinical course of heterozygous miR-142 mice was ameliorated by peripheral DMF treatment with a greater impact relative to their wild type littermates. In addition, a central protective effect of this drug was observed following intracerebroventricular and ex vivo acute treatments of EAE wild type mice, showing a rescue of miR-142-3p-dependent glutamatergic alterations. By means of electrophysiology, molecular and biochemical analysis, we suggest miR-142-3p as a molecular target of DMF.

Conclusion: MiR-142-3p is a novel and potential negative prognostic CSF marker of MS and a promising tool for identifying personalised therapies.

KEYWORDS
biological marker, experimental autoimmune encephalomyelitis, fumarates, microRNA, multiple sclerosis, synaptopathy

INTRODUCTION

Multiple sclerosis (MS) is a chronic immune-mediated demyelinating and neurodegenerative disease, characterised by the infiltration of activated T and B cells into the CNS and by compartmentalised CNS inflammation.[1,2] In most patients, the disease begins with a relapsing–remitting course (RRMS), which may subsequently convert into a secondarily progressive one (SPMS). However, a minority of patients show a continuous progressive deterioration of neurological function from the beginning, without distinct relapses (attacks or exacerbations) or remission (primary progressive course, PPMS). Clinical classification also provides clinically isolated syndrome (CIS), a single clinical event resembling MS that could evolve in a relapsing–remitting disease course or remain isolated, and radiologically isolated syndrome (RIS), an incidental finding of radiological signs of disease in the absence of clear clinical activity.[3] Disease progression is a feature of MS from the very beginning of the condition. This is supported by the evidence that cognitive changes appear very early,[4] brain volume loss starts from the stage of CIS[5] and progression independent of relapses (PIRA) seems to be a dominant disability accrual factor even in early and RRMS patients.[6] The clinical presentation and the disease course of MS are highly variable, reflecting the heterogeneity of pathophysiology. Accordingly, demyelination, axonal damage, inflammatory synaptopathy and neurodegeneration may contribute in different proportions and coexist with reparative processes.[1,2,7] Therefore, understanding the roles of different pathogenic mechanisms, and the identification of pivotal molecular players involved in the disease pathogenesis and progression, is crucial to design effective therapeutic interventions in MS.

Key points

- miR-142-3p is a potential negative prognostic CSF marker of MS disease and may influence the efficacy of dimethyl fumarate therapy
- CSF MiR-142-3p levels of MS patients positively correlate with IL-1β signalling and neuronal excitability in MS patients
- IL-1beta/miR-142-3p/GLAST regulatory axis drives synaptopathy in the EAE mouse model and is dampened by fumarate treatments targeting miR-142-3p

Small noncoding microRNAs (miRNAs or miR) are an important class of molecules critically involved in modulating gene expression and are considered sensitive biomarkers and potential therapeutic targets for many diseases.[8,9] Notably, altered expression of various miRNAs (including, miR-155 and miR-21) have been detected in the peripheral blood, CSF and brain tissue of MS patients and in one of

the most widely used animal model of MS, experimental autoimmune encephalomyelitis (EAE).[10,11] It has been shown that different therapeutic approaches may modulate the expression and activity of specific miRNA and particularly of miR-142-3p.[12–14] MiR-142-3p and its isoform miR-142-5p have been reported in the list of those miRNAs of the immune system[15–21] potentially involved in MS and EAE pathogenesis and that may be useful as diagnostic markers for MS.[10,17,22,23] Accordingly, increased miR-142-3p has been found in MS white matter lesions and in lesioned area of EAE brain.[14,17,23–27] We have previously demonstrated that miR-142-3p is overexpressed in the CSF of RRMS patients and in the cerebellum of EAE mice. In particular, we proposed miR-142-3p as a potential molecular player in MS disease progression promoting inflammatory synaptopathy,[28] a distinctive hallmark of MS recently identified in the context of grey matter pathology.[7,29,30]

Synaptopathy consists of a diffuse synaptic dysfunction and synaptic loss in the CNS that later on can cause excitotoxic damage and neuronal death. It has been demonstrated that synaptopathy is crucially mediated by several inflammatory molecules released by infiltrating lymphocytes and resident immune cells and may represent, at least in the initial stages, a reversible process.[7,28,31,32] In EAE cerebellum, miR-142-3p is highly expressed and acts downstream of the proinflammatory cytokine IL-1β to repress posttranscriptionally the glial glutamate–aspartate transporter (GLAST). In this way, miR-142-3p impairs the reuptake of glutamate from the synaptic cleft, leading to an increase in the duration of excitatory postsynaptic currents and later on to excitotoxicity. Furthermore, we showed that CSF of MS patients carrying high miR-142-3p levels is able to induce synaptopathy when incubated with murine brain slices (CSF chimeric ex vivo MS model), mimicking the synaptic dysfunction seen in EAE. Consistently, coincubation with a miR-142-3p inhibitor normalised the synaptic alterations evidenced in the chimeric model, confirming the potential role of this molecule in promoting disease progression.[28]

Here, we explored the clinical impact of CSF miR-142-3p levels in a large cohort of MS patients. In particular, we investigated the potential role of miR-142-3p as a negative prognostic marker, its association with IL-1β signalling, its potential impact on synaptic excitability and its interaction with therapeutic treatment through both clinical and preclinical studies.

MATERIALS AND METHODS

Clinical study design

This observational prospective study was carried out in compliance with the Declaration of Helsinki principles and was approved by the Institutional Review Board (NCT03217396 recorded in https://clinicaltrials.gov/) of the IRCCS Istituto Neurologico Mediterraneo (INM) Neuromed in Pozzilli (Isernia, Italy). All subjects provided their written informed consent. All details are provided in the Supporting Information.

RNA extraction from CSF and miR-142-3p detection

Briefly, after the collection of CSF samples (0.5–2 ml), cellular elements were removed immediately by centrifugation (1300 rpm: 189 G-force, 10 min) and supernatants were stored at −80°C. RNA extraction and qPCR experiments were performed as described in Mandolesi et al., 2021.[33] As endogenous reference for the ΔCt calculation (Ct miR-142-3p–Ct miR-204-5p), we used miR-204-5p. Low ΔCt-values indicate high miR levels and data are presented as 2^(−ΔCt).[28,33] All details are provided in the Supporting Information.

Biochemical parameter detection in human CSF

Custom multiplex kits, designed to simultaneously measure multiple protein targets in a single sample, were used (R&D systems) to screen IL-1β and interleukin-1β receptor antagonist (IL-1ra) levels in the CSFs withdrawn from recruited subjects. Proteins below the detection sensitivity of the standard curve (< 0.01 pg/ml) were considered as 0 pg/ml.

Transcranial magnetic stimulation (TMS)

TMS was performed in a subgroup of 20 patients with MS, asymptomatic in the right upper limb. Paired pulse TMS was performed to assess synaptic excitability. A detailed protocol is provided in the Supporting Information. All patients gave written informed consent to the procedure. No patients were treated with corticosteroids or other disease-modifying treatments (DMTs) before TMS.

Mice, EAE induction and treatment protocols

Both female heterozygous (HE +/−) and homozygous knock-out (KO −/−) miR-142-deficient C57BL/6 LacZ gene knock-in mice[20] with related wild-type (WT +/+) littermates were used for all the experiments. Animal experiments described in this study were conducted according to the guidelines set by the Internal Institutional Review Committee, the European Directive 2010/63/EU and the European Recommendations 526/2007 and the Italian D. Lgs 26/2014.

EAE was induced in 8- to 10-week-old mice by active immunisation with an emulsion of myelin oligodendrocyte glycoprotein peptide 35-55 (MOG35-55) in Complete Freund's Adjuvant (CFA), followed by intravenous administration of pertussis toxin (500 ng) twice (at days 0 and 2) as previously described.[28,34] As controls animals received the same treatment as EAE mice without the immunogen, MOG peptide, including complete CFA and Pertussis toxin (referred to as 'CFA').

Animals were scored daily for clinical symptoms of EAE according to a 0–5 scale.[28,34] All efforts were made to minimise the number of animals used and their suffering.

The following treatments were performed: preventive peripheral treatment (0-day postimmunisation, dpi) with dimethyl fumarate

(DMF) (60 mg/kg/day; Sigma-Aldrich); therapeutic peripheral treatment (at onset, 10–14 dpi) with DMF; central therapeutic treatment (21–25 dpi, twice 24 hours apart) with monomethyl fumarate (MMF, 0.325 mg/kg/day).

Details of animal housing, EAE symptoms evaluation and treatments are provided in the Supporting Information.

Electrophysiology

Mice were sacrificed by cervical dislocation and cerebellum slices (210 μm) were prepared from fresh tissue blocks of the brain with the use of a vibratome. Briefly, after 1 h of recovery time in a chamber containing oxygenated artificial cerebrospinal fluid (ACSF), spontaneous excitatory post synaptic currents (sEPSCs) were recorded from Purkinje cells (PCs) by means of whole cell patch-clamp technique in the presence of bicuculline. Spontaneous synaptic event recording, data storing, and analysis were performed as previously described.[28] One to six cells per animal were recorded.

For ex vivo experiments, brain slices from EAE mice in the acute phase of the disease (20–25 dpi) were incubated for one or 2 h in ACSF with MMF (100 μM, Sigma-Aldrich) or vehicle (PBS-DMSO 0.001% final concentration).

Flow cytometry

Spleen cells were recovered from all the different groups of mice. Fluorescence-activated cell sorting (FACS) staining and analysis (FACSCanto II; BD Biosciences) of splenocytes were performed by FACSDiva (BD) and FlowJo (Tree Star) software was used for the analyses. Antibody list is in the Supporting Information.

Cerebellar slice preparation, real time PCR (qPCR) and Western blot (WB) analysis

Cerebellar slices (210 μm) from EAE mice in the acute phase of the disease (20–25 dpi) were incubated for 2 h with MMF (100 μM, Sigma-Aldrich) or vehicle (PBS-DMSO 0.001% final concentration). Incubations with the following compounds were also performed: TAT-14 Peptide, (75 μM, Calbiochem in PBS), actinomycin D (25 μM; Sigma-Aldrich in DMSO 2.5% final concentration) or respective vehicle (VEH).

For qPCR experiments, total RNA was extracted as previously described[28] and the expression of miR-142-3p, *Tnf*, *Ho-1*, Cd3 and *Aif1* mRNA coding for IBA-1 was evaluated by using TaqMan technology according to Applied Biosystems' instructions. SensiMix SYBR Hi-Rox Kit (Bioline; Meridian Life Science) was used for the detection of *Slc1a3* mRNA coding for GLAST, IL-1β mRNA and *glial fibrillary acidic protein* (GFAP) mRNA. Both miRNA and mRNA relative quantifications were performed using the comparative cycle threshold ($2 - \Delta\Delta Ct$) method. U6B β-actin was used, respectively as endogenous control. qPCR details are in the Supporting Information and primers used are listed in Table S1.

For WB analysis, slices were homogenised in RIPA buffer plus protease inhibitor mixture (Sigma-Aldrich) and sonicated. WB experiments were performed as previously described[28] and results were presented as data normalised to control values.

Statistics

Statistical analysis was performed with Prism GraphPad 6.0 and IBM SPSS Statistics 17.0. Data distribution was tested for normality by using Kolmogorov–Smirnov test and Shapiro–Wilk test. Correlation between miR-142-3p CSF levels and, demographic and clinical parameters were made by nonparametric Spearman correlation analysis. Differences between two groups were analysed using two-tailed Student's *t* test, Mann–Whitney U test and Fisher's exact test, as appropriate. Multiple comparisons were performed by ANOVA followed by Tukey HSD. Data were presented as the mean ± S.E.M, unless otherwise specified. The significance level was established at $p < 0.05$.

RESULTS

MiR-142-3p levels in the CSF of MS patients associate with disease progression, IL-1β signalling and excitability in patients with MS

We evaluated by qPCR analysis the levels of miR-142-3p in the CSF of a cohort of 151 patients with MS (clinically or radiological isolated syndrome, CIS/RIS, $n = 18$; RRMS, $n = 108$; PMS, $n = 25$) and control subjects (CTRL, $n = 20$) to perform correlation analysis with clinical and demographic parameters recorded at the time of CSF withdrawal (T0) (Figure 1A, Table 1). We observed a positive correlation between CSF miR-142-3p levels and the Progression Index (PI(T0)) of patients with MS ($n = 151$, $p < 0.01$; Figure 1B), while no significant associations were observed for the other clinical or demographic parameters examined (disease duration, Expanded Disability Status Scale [EDSS], sex, age; Table 1). We also evaluated the PI(T0) in two subgroups of MS patients—the 'Low miR-142-3p' group (Low, $n = 75$) and the 'High miR-142-3p' group (High, $n = 76$)—identified using the median value of the CSF miR-142-3p levels as cut-off (0.010; Table 1). In accordance with the correlation analysis, we observed a significant difference of PI(T0) between the two subgroups ($p < 0.01$; Figure 1C and Table S2).

In the same group of patients, we investigated a potential association between CSF miR-142-3p levels and IL-1β signalling, to support the relevance of the IL-1β-miR-142-3p axis in EAE/MS synaptopathy.[28] Although most subjects carried undetectable level of IL-1β in the CSF (Table 1), we observed a positive correlation between CSF miR-142-3p and IL-1β at T(0) in MS patients (Figure 2A; $n = 151$, $p < 0.01$) and no association in the control group ($p > 0.05$, Table 1). Accordingly, the amount of miR-142-3p was significantly different between patients with 'no-detectable' and 'detectable' levels of IL-1β

TABLE 1 Demographic and clinical characteristics of control subjects and all MS patients at CSF withdrawal (T0)

			Patients' groups		
Variable	**Control subjects**	**All patients**	**CIS/RIS**	**RRMS**	**PMS**
N	20	151	18	108	25
Gender (F/M)	13/7	97/54	15/3	71/37	11/14
Age (yr)	42.574 ± 15.434	39.51 ± 12.27	36.330 ± 13.96	39.34 ± 12.13	42.55 ± 11.38
Disease activity (y/n/NA)	--	61/75/15	9/9/0	40/63/5	12/3/10
CSF oligoclonal banding (y/n/NA)	--	117/26/8	4/13/1	18/84/6	4/20/1
Disease duration (mos)	--	12.430 (2.400–39.270)	2.765 (1.000–6.928)	12.920 (1.705–46.420)	24.700 (12.000–61.650)
EDSS (score 0–10)	--	2.000 (1.000–3.000)	1.500 (1.000–2.125)	1.750 (1.000–3.000)	3.500 (2.250–5.500)
CSF miR-142-3p ($2^{\wedge(-\Delta Ct)}$ rel. to miR-204-5p)	0.006 (0.004–0.010)	0.010 (0.004–0.020)	0.009 (0.001–0.014)	0.010 (0.004–0.023)	0.009 (0.005–0.015)
IL-1β (all values; pg/ml)	0.000 (0.030–0.070)	0.000 (0.000–0.060)	0.000 (0.000–0.015)	0.000 (0.000–0.060)	0.000 (0.000–0.060)
IL-1β (detected values; pg/ml)	0.050 (N = 13) (0.030–0.075)	0.060 (N = 70) (0.030–0.100)	0.070 (N = 5) (0.020–0.070)	0.060 (N = 52) (0.032–0.110)	0.060 (N = 13) (0.025–0.09)
IL-1β/IL-1ra ratio (all values)	0.001 (0.000–0.003)	0.000 (0.000–0.004)	0.000 (0.000–0.000)	0.000 (0.000–0.004)	0.000 (0.000–0.004)
IL-1β/IL-1ra ratio (detected values)	0.002 (N = 13) (0.001–0.003)	0.004 (N = 70) (0.002–0.012)	0.003 (N = 5) (0.002–0.021)	0.004 (N = 52) (0.002–0.013)	0.003 (N = 13) (0.001–0.011)
PI(T0) (EDSS score/mos)	--	0.162 (0.028–0.682)	0.524 (0.073–1.287)	0.137 (0.021–0.700)	0.160 (0.043–0.300)

Note: Age is mean ± standard deviation. Other data are median and 25th–75th percentiles. All patients have been considered and divided in relapsing–remitting MS (RRMS), progressive MS (PMS) and clinically isolated syndrome-radiological isolated syndrome (CIS/RIS).
Abbreviations: CSF, cerebrospinal fluid; EDSS, Expanded Disability Status Scale; F, female; M, male; mos, months; y/n/NA, yes/no/not available; yr, year; IL-1β/IL-1ra ratio, ratio between interleukin-1β and interleukin-1β receptor antagonist; PI(T0), Progression Index at T0.

($p < 0.01$ Figure 2B), in line with the miR-142-3p cut-off value previously identified (Table 1).

We looked also at the ratio between the CSF levels of IL-1β and its endogenous inhibitor IL-1 receptor antagonist (IL-1β/IL-1ra, the actual functional activity of IL-1β), previously associated with neurotoxic hyperexcitability in MS.[35] We found that CSF miR-142-3p directly correlated with the CSF levels of IL-1β/IL-1ra ($n = 151$, $p < 0.01$; Figure 2C) and MS patients carrying high levels of both members of this regulatory axis showed a worse PI in comparison to subgroups with low levels of miR-142-3p and/or IL-1β/IL-1ra ratio ($p < 0.05$ L/(-) –L/(+) –H/(-) $n = 107$ vs. H/(+) $n = 44$; Figure 2D).

Finally, to explore the impact of miR-142-3p CSF levels on synaptic excitability in MS patients, we assessed glutamatergic synaptic transmission by intermittent theta burst stimulation (iTBS) in a subgroup of 20 MS patients (Table S3). The TMS protocol was well tolerated in all patients and no adverse effects were reported. In line with the electrophysiological experiments in EAE model, a direct correlation emerged between miR-142-3p CSF levels at (T0) and the increase of corticospinal excitability induced by iTBS after 15 minutes and 30 minutes ($p < 0.05$; Figure 2E), independently of clinical and demographic parameters (EDSS, age). No significant associations were observed between the TMS parameters analysed and IL-1β or IL-1β/IL-1ra ratio. These results suggest that miR-142-3p might interfere with synaptic excitability in patients with MS.

Altogether, these results highlight the relevance of the IL-1β-miR-142-3p axis, in particular of miR-142-3p in MS synaptopathy and its impact on disease progression.

Implications of CSF miR-142-3p levels on the efficacy of disease-modifying treatments (DMTs) for MS: the possible impact on therapeutic response to dimethyl fumarate

Considering the influence of CSF miR-142-3p levels on MS disease progression, we explored a possible interaction between miR-142-3p and DMTs currently used to treat MS. We first identified a subcohort of patients that received platform drugs (I-line DMTs, $n = 105$) and confirmed a positive correlation between CSF miR-142-3p levels and PI(T0) ($p < 0.01$; Figure 3A). We stratified these patients in 'High' and 'Low miR-142-3p' subgroups as previously described and, coherently with the results obtained on the whole cohort, we observed that patients with 'High levels of miR-142-3p' showed a more severe PI(T0) ($n = 47$) in comparison to subjects with 'Low levels' ($n = 58$, $p < 0.01$; Figure 3B and Table S2). In order to explore a potential

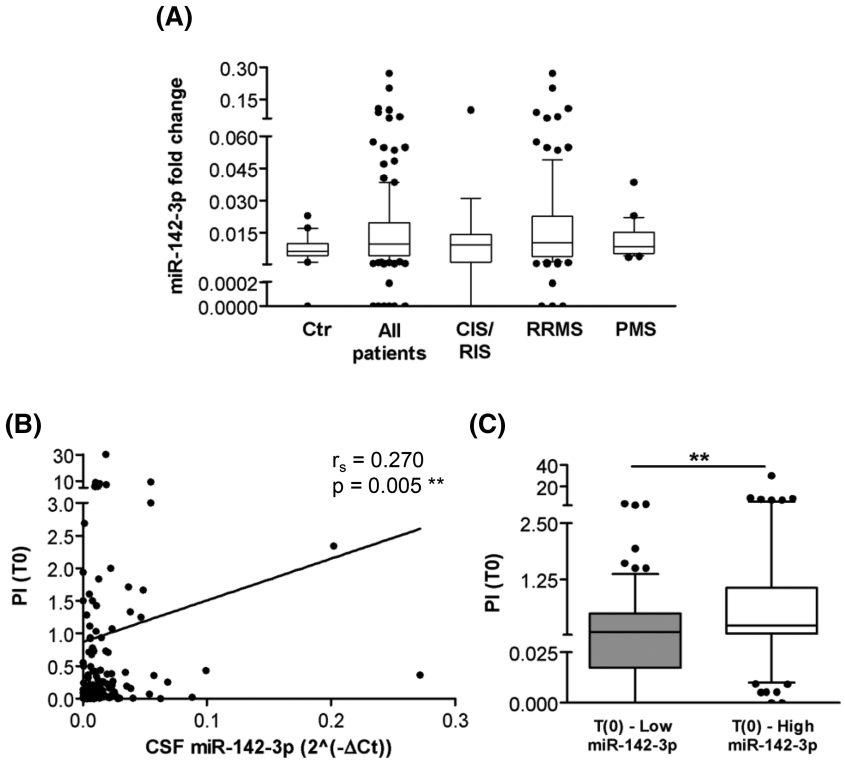

FIGURE 1 MiR-142-3p levels in the CSF associate with MS severity. (A) Box-and-whisker plots of miR-142-3p levels in the CSF isolated from control subjects (Ctr) compared to all patients (Ctr, $n = 20$; all patients, $n = 151$; Mann–Whitney test, $p > 0.05$) or to patients separated in clinically/radiological isolated syndrome (CIS/RIS), relapsing–remitting MS (RRMS) and progressive MS (PMS) (Ctr, $n = 20$; CIS/RIS, $n = 18$; RRMS, $n = 108$; PMS, $n = 25$; one-way ANOVA, $p > 0.05$). Data were normalised to miR-204-5p using the ΔCt calculation ('$Ct_{miR\text{-}142\text{-}3p}$'–'$Ct_{miR\text{-}204\text{-}5p}$'). Values are median (—) of $2^{\wedge(-\Delta Ct)}$ with 10–90% percentiles (error bars) and 25–75% percentiles (open boxes). (B) Correlation plot between CSF miR-142-3p levels ($2^{\wedge(-\Delta Ct)}$ relative to miR-204-5p) and the progression index at the withdrawal (PI(T0)). A positive correlation was observed ($n = 151$, Spearman correlation, Spearman's $r = 0.216$, $p < 0.01$). (C) Box-and-whisker plots of the progression index (PI) of the disease in patients with low ($n = 75$) and high ($n = 76$) levels of miR-142-3p ($2^{\wedge(-\Delta Ct)}$ relative to miR-204-5p) at the withdrawal (PI(T0); the high miR-142-3p group presented at T0 a worse PI relative to the low group (Mann Whitney test, $p < 0.01$)

interaction between miR-142-3p and a specific DMT, we explored in both 'Low' and 'High' subgroups the proportion of patients that switched to II-line treatments because of disease reactivation. We identified subjects treated with the moderate efficacy I-line drug DMF[36,37] as the more appropriate group for this type of analysis in terms of number of patients (Low: $n = 24$; High: $n = 24$) and PI associated with miR-142-3p subgroups ($p < 0.05$; Figure 3C, Table S2). We observed that following 2.5 years of DMF treatment, 100% of the 'Low miR-142-3p' patients remained stable, while 25% of the High subjects switched to a second therapy ($p < 0.05$; Figure 3D), indicating a potential interaction between the amount of miR-142-3p and DMF treatment.

Altogether, these results highlight the efficacy of a stratification of MS patient in 'Low' and 'High' miR-142-3p subgroups as potential indicator of disease severity and response to therapy.

EAE miR-142 HE mice are more sensitive to DMF preventive peripheral treatment

The results obtained from the analysis of the CSF patients support a role for miR-142-3p in contributing to MS pathological processes, likely contributing to neuronal dysfunction, and suggest that miR-142-3p is a possible target of DMF, a I-line therapy with both immunomodulatory and neuroprotective effects. To investigate further the interaction between miR-142-3p and DMF, we performed additional experiments in the EAE model. Notably, miR-142 knockout mice (miR-142 KO mice) are resistant to EAE induction,[28] therefore, we characterised miR-142 heterozygous mice (miR-142 HE) at both central and peripheral levels, and induced $MOG_{(35-55)}$ EAE in these mice (Figure S1). We observed that naïve miR-142 HE mice, despite having at basal level a reduced relative proportion of $CD3^+$ and $CD4^+$ cells within the circulating $CD45^+$ population in the spleen (Figure S1C–E) and no differences in regulatory T cell (Treg) compartment, were as fully responsive to EAE induction as their WT littermates (Figure S1A, B). Furthermore, EAE miR-142-HE mice were protected at the synaptic level, in terms of glutamatergic synaptic alteration in the EAE cerebellum (Figure S1F,G), in accordance with our previous observations.[28]

To verify then the effect of DMF on EAE mice carrying different amount of miR-142-3p, miR-142-HE mice as well as WT mice were intraperitoneally (ip) injected with DMF or vehicle, starting from the day of immunisation (0 dpi) until the acute phase of the disease (21–

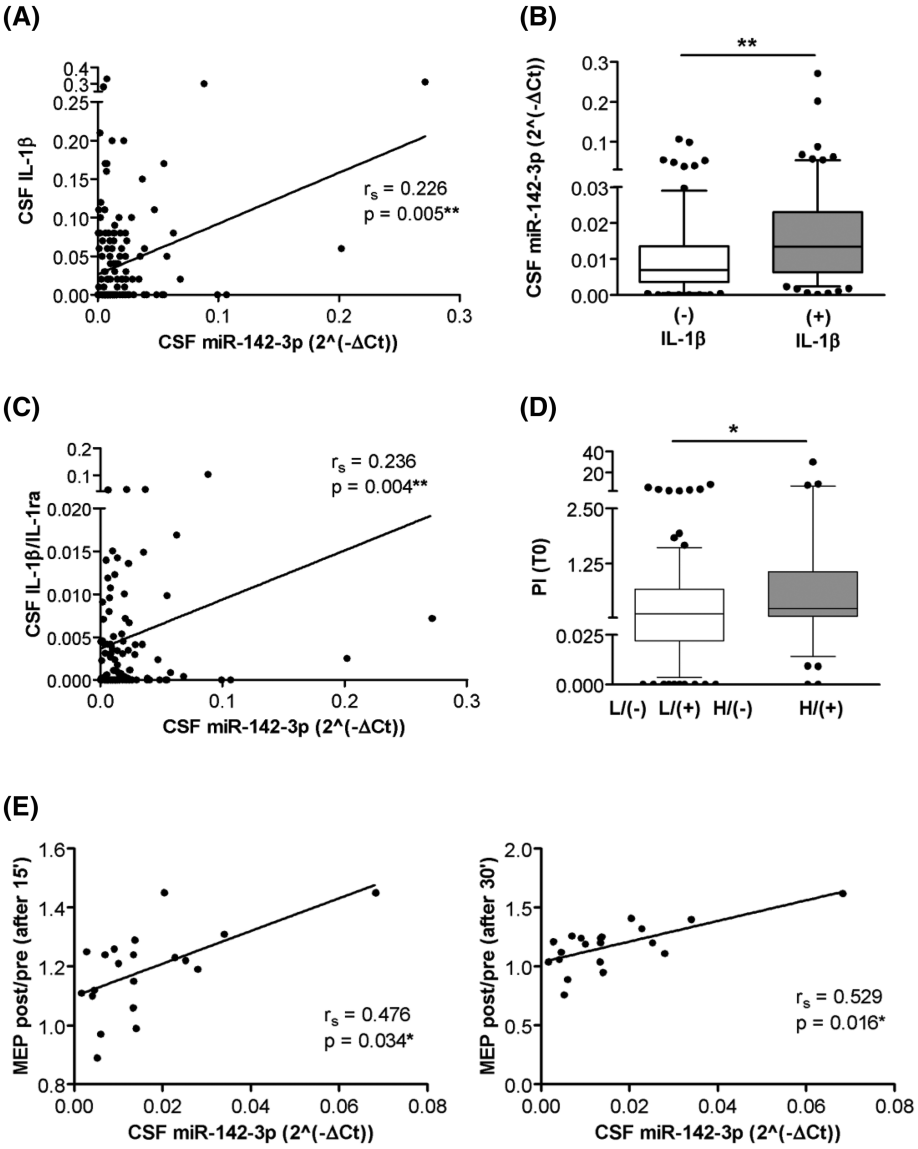

FIGURE 2 MiR-142-3p levels in the CSF associate with central inflammation and neuronal hyperexcitability. (A) Correlation plot between miR-142-3p and interleukin-1β (IL-1β) levels circulating in the CSF of all patients with MS at the withdrawal. A positive correlation is observed (T0; $n = 151$, Spearman's: $r = 0.226$, $^{**}p < 0.01$). (B) Box-and-whisker plots of CSF miR-142-3p at the withdrawal (PI(T0)) in patients with undetectable (−) and detectable (+) levels of IL-1β (white box: -; grey box: +); Mann Whitney test, $p < 0.01$). (C) Correlation plot between miR-142-3p and interleukin-1β/IL-1 receptor antagonist ratio (IL-1β/IL-1ra ratio) quantified in the CSF isolated from all MS patients at the withdrawal. A positive correlation is observed (T0; $n = 151$, Spearman's: $r = 0.236$, $^{**}p < 0.01$). (D) Box-and-whisker plots of the progression index at the withdrawal (PI(T0)) in patients with high (H, miR-142-3p ≥ 0.01) or low (L, miR-142-3p < 0.01) levels of miR-142-3p and detectable (+) or undetectable (−) IL-1β/IL-1ra ratio (white box: L/+, L/−, H/−; grey box: H/+; Mann Whitney test, $^{*}p < 0.05$). Median values of miR-142-3p, IL-1 β and IL-1β/IL-1ra ratio were used as respective thresholds. (E) MiR142–3p levels directly correlate with neuronal excitability; correlation plot between CSF miR-142-3p levels and the mean amplitudes of motor-evoked potentials (MEP post, normalised to the mean baseline MEP, MEP pre) evaluated at T0 in a subgroup of patients ($n = 20$) after 15 min (left, Spearman's: $r = 0.476$, $^{*}p < 0.05$) and 30 min (right, Spearman's $r = 0.529$, $^{*}p < 0.05$) from an intermittent theta burst stimulation (iTBS). MiR-142-3p levels in CSF are calculated as $2^{\wedge(-\Delta Ct)}$ relative to miR-204-5p

28 dpi). DMF was more effective in improving motor disability in EAE-HE mice than in EAE-WT mice (Figure 4A), unveiling a synergistic effect of fumarate and miR-142 heterozygosis condition. To explore a potential DMF-miR-142 interaction at the peripheral level, we performed a profiling of the T cells in the four experimental groups (Figure 4B–D). We found that DMF treatment did not alter the frequency of $CD3^+$ T cells in both WT and HE mice, whereas it reduced to similar extent the relative proportion of $CD8^+$ T cells (within $CD3^+$ cells DMF vs. VEH; WT: $p < 0.05$; HE: $p < 0.01$), paralleled by a compensatory increase of $CD4^+$ percentage in the spleens (within $CD3^+$ cells DMF vs. VEH; WT: $p > 0.5$; HE: $p > 0.5$). Interestingly, DMF displayed an inhibitory effect on the B cell compartment ($B220^+$ cells), selectively in HE mice, with no effects on WT mice (DMF vs. VEH; WT: $p > 0.5$; HE: $p < 0.01$). Regarding the regulatory T (Treg) cell

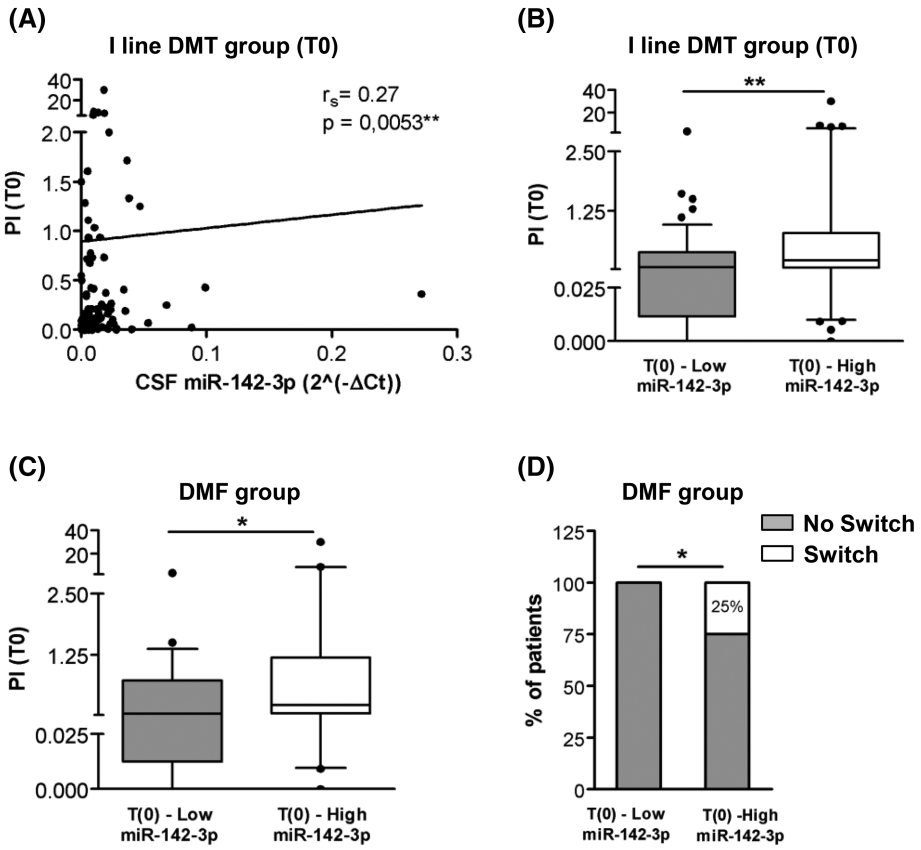

FIGURE 3 MiR-142-3p levels in the CSF might influence the therapeutic response to DMF. (A) Correlation plot between CSF miR-142-3p levels and the Progression Index at the withdrawal (PI(T0)). A positive correlation was observed ($n = 105$, Spearman correlation, Spearman's $r = 0.270$, $p < 0.01$). (B) Box-and-whisker plots of the PI of patients treated with I-line therapy. The PI(T0) was more severe in the High miR-142-3p group compared to the Low group (Low: $n = 58$, High: $n = 47$; Mann Whitney test, $p < 0.01$). (C) Box-and-whisker plots of the progression index (PI) of patients treated with DMF. The PI(T0) was more severe in the High miR-142-3p group compared to the Low group (Low: $n = 24$, High: $n = 24$; Mann Whitney test, $p < 0.05$). (D) The histograms show the percentage of DMF treated patients of the two miR-142-3p subgroups that switched to a second therapy. The patients of the Low miR-142-3p group were better responders to DMF in comparison to patients of the High group (Low: $n = 24$, $n = 24$ No Switch, $n = 0$ Switch; High: $n = 24$, $n = 18$ No Switch, $n = 6$ Switch; Fisher's exact test, $p < 0.05$). MiR-142-3p levels in CSF are calculated as $2^{\wedge(-\Delta Ct)}$ relative to miR-204-5p. Statistical values, $^{*}p < 0.05$, $^{**}p < 0.01$

compartment involved in the maintenance of immunological tolerance, we found an increased frequency of Treg cells (evaluated as $CD4^{+}Foxp3^{+}$ cells) in spleens of DMF-treated mice, regardless of the genotype (DMF vs. VEH; WT: $p < 0.01$; HE: $p < 0.01$, Figure 4C). However, DMF was able to increase the expression of a series of markers associated with Treg cell suppressive function/proliferation (such as PD-1, GITR, CTLA-4, CD69, Helios or Ki67), selectively in HE mice (Figure 4C,D), thus suggesting that Treg cells from these mice were more sensitive than WT Treg cells to the immune modulation induced by DMF and were possibly more capable to control autoreactivity.

EAE synaptopathy is improved by DMF peripheral and MMF central treatment

To explore the therapeutic efficacy of a potential DMF-miR-142 interaction at the central level, we investigated the effect of DMF on the miR-142-3p–mediated glutamatergic alterations observed in EAE cerebellum.[28] To this end, we treated EAE WT mice during the symptomatic phase of the disease, with DMF or its active metabolite, MMF, by following a peripheral or a central approach, respectively. First, we observed that daily peripheral treatment with DMF starting from the day of onset (10–14 dpi), was able to mitigate the enhancement of the duration of the sEPSCs recorded from PCs in EAE cerebellum (decay time EAE-VEH vs. EAE-DMF $p < 0.05$; Figure 5A). As expected, such DMF treatment also significantly ameliorated the clinical score in EAE mice during the acute phase of the disease (Two-way ANOVA: EAE-VEH: $n = 10$; EAE-DMF: $n = 18$; $F = 46.90$, $df = 15$, $p < 0.01$ at 19–20 dpi; data not shown). Then, to verify a direct neuroprotective effect of the drug, MMF or vehicle were delivered, by means of an acute intracerebroventricular administration, in symptomatic EAE mice (21–25 dpi) for two consecutive days, 24 h apart (Figure 5B). After 1 h from the infusion, electrophysiological experiments showed that the sEPSC decay time recorded from PCs was significantly reduced in MMF-EAE mice, compared with EAE vehicle mice ($p < 0.05$), with values similar to those of control mice

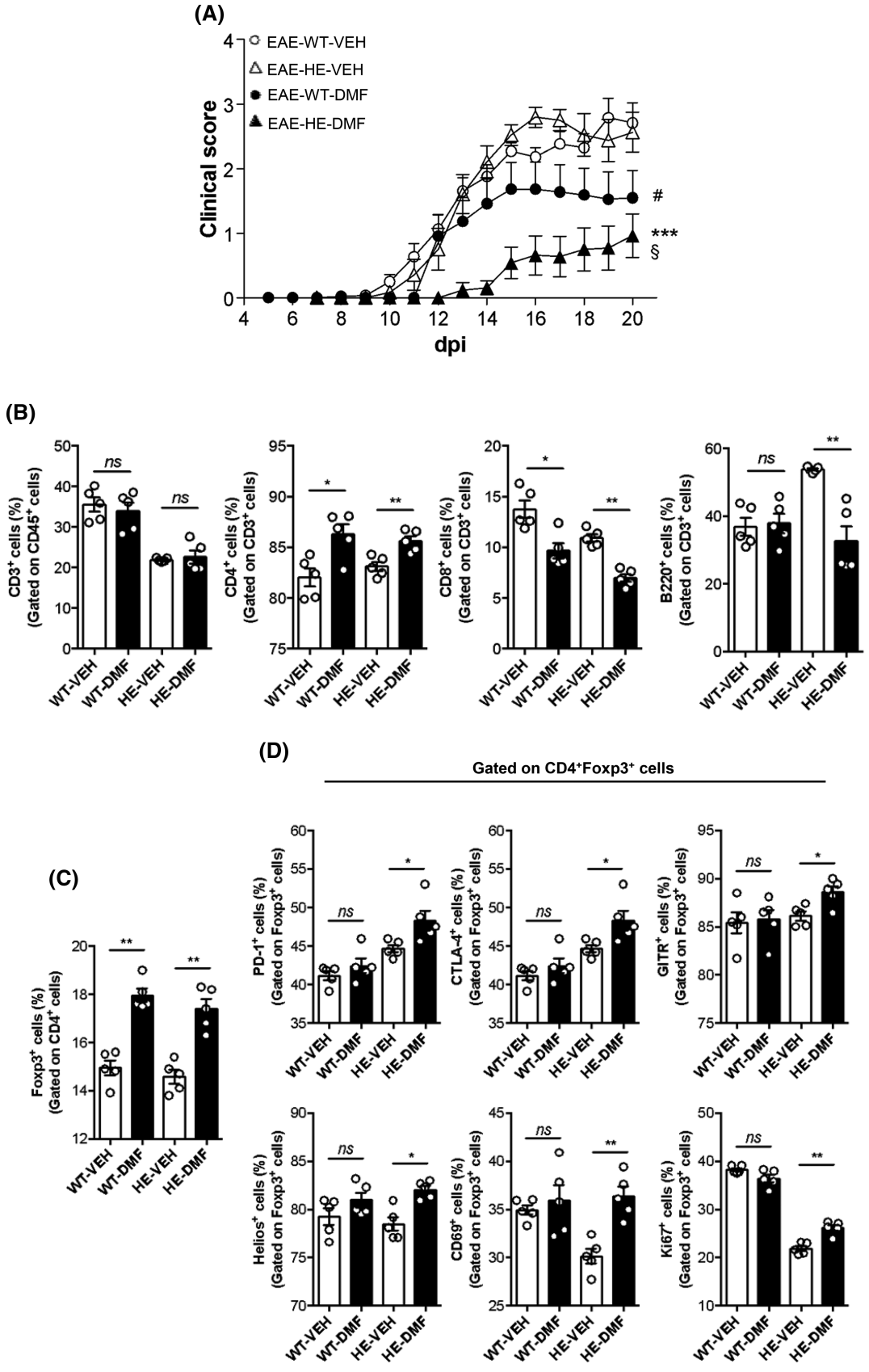

FIGURE 4 Legend on next page.

FIGURE 4 Synergistic effect between DMF preventive treatment and miR-142 in heterozygous miR-142 mice. (A) Dot plots showing the time course of clinical score in EAE-WT-VEH (white circles), EAE-WT-DMF (black circles), EAE-HE-VEH (white triangles) and EAE-HE-DMF (black triangles) mice. A preventive (0 dpi) and peripheral DMF treatment (i.p., 60 mg/kg/day) was more effective in improving motor disability in EAE-HE mice than in EAE-WT mice (EAE-WT VEH $n = 28$; EAE-HE VEH: $n = 12$; EAE-WT DMF: $n = 11$; EAE-HE DMF: $n = 13$; two-way ANOVA followed by Tukey HSD: DMF vs. VEH in EAE WT mice, $p < 0.05$ #; DMF vs. VEH in EAE-HE mice, $p < 0.001^{***}$; HE vs. WT in DMF, $p < 0.05$§). Data are from one representative immunisation (n immunisation $= 2$). (B) Flow cytometry analysis of spleen cells from EAE-WT and EAE-HE mice treated or not with DMF, showing the percentages (%) of $CD3^+$, $CD4^+$, $CD8^+$, $B220^+$ cells. Data are expressed as mean ± SEM and each symbol represents a single mouse. (C,D) Flow cytometry analysis of Treg cells (evaluated as $CD4^+Foxp3^+$ cells) in spleens of the different groups of mice. Histograms indicate the percentages (%) of (C) $Foxp3^+$ cells and the percentages (%) of (D) $PD1^+$, CTLA-4^+, $GITR^+$, $Helios^+$, $CD69^+$ and $Ki67^+$ cells gated on $CD4^+Foxp3^+$ cells. Data are expressed as mean ± SEM and each symbol represents a single mouse ($n = 5$ mice/group); statistical analysis are performed by using Mann–Whitney U test (two tails); $^*p < 0.05$; $^{**}p < 0.01$; ns, not significant

(Figure 5B). The effect of MMF on the half-width was less remarkable (Figure 5B). Finally, to further validate a direct action of the drug on the CNS, MMF or vehicle were ex vivo applied on cerebellar EAE slices (20–25 dpi). Notably, 2 h of MMF bath application completely prevented the alteration of the sEPSC decay time and half width, recorded from EAE PCs in comparison to vehicle treated ones (both decay time and half width $p < 0.001$; Figure 5C).

These results clearly indicate that prolonged therapeutic treatment with DMF as well as acute central administration or ex vivo incubation of MMF were sufficient to ameliorate cerebellar glutamatergic alterations in EAE mice, revealing a novel antisynaptotoxic action of fumarates.

Fumarates ameliorate glutamatergic transmission in EAE cerebellum by interfering with miR-142-3p-GLAST/EAAT1 regulatory axis

To provide a mechanistic explanation of the beneficial effect provided by MMF treatment on EAE cerebellar synaptopathy, we considered the involvement of IL1-β-miR-142-3p-GLAST/EAAT1 axis.[28] As shown in Figure 6, 2-h incubation of MMF on EAE cerebellar slices was able to increase the expression of Slc1a3, the mRNA coding for the glial transporter GLAST/EAAT1 (EAE-VEH vs. EAE-MMF: $p < 0.01$; Figure 6A), as well as to restore the protein level (EAE-VEH vs. EAE-MMF: $p < 0.05$; Figure 6A), supporting the functional improvement of the glutamatergic transmission. Interestingly, MMF incubation was able to reduce miR-142-3p expression (EAE-VEH vs. EAE-MMF: $p < 0.05$; Figure 6B), without changing IL1-β mRNA levels (Figure 6C), suggesting that MMF increased the GLAST/EAAT1 translation by directly acting on miR-142-3p, downstream IL-1β, in the IL-1β-miR-142-3p-GLAST/EAAT1 pathway. Neither other pro-inflammatory cytokines, like TNF (Figure 6C) nor other markers of neuroinflammation, including GFAP for astrogliosis, IBA1 for microgliosis and Cd3 for lymphocyte infiltrates were affected by acute incubation with MMF (Figure S2A–C).

We then assessed whether MMF could downregulate miR-142-3p expression through activation of the transcription factor Nuclear factor (erythroid-derived 2)-like (Nrf2), a well-known mediator of the drug signalling.[38,39] To address this question, we evaluated the mRNA levels of Heme oxygenase (Ho-1), which is one of the principal target gene of Nrf2,[40] in EAE cerebellar slices following 2-h incubation with MMF. qPCR results showed that Ho-1 expression was not enhanced by MMF in our experimental condition (EAE-VEH vs. EAE-MMF: $p > 0.05$; Figure 6D). In accordance with this result, neither the miR-142-3p level nor the Ho-1 mRNA levels (Figure S3A, B) were modulated by acute incubation with the Nrf2 activator TAT-14.[40]

To understand whether MMF interferes with miR-142-3p expression at the transcriptional level, we performed 2-h incubation of MMF combined with the transcriptional inhibitor actinomycin D on EAE cerebellar slices and quantified miR-142-3p by qPCR in four experimental conditions. Specifically, EAE slices were ex vivo incubated with vehicle (CTR-EAE-VEH) or MMF alone (CTR-EAE-MMF) and together with actinomycin D (ACT-EAE-VEH and ACT-EAE-MMF). One-way analysis of variance confirmed miR-142-3p down-regulation mediated by MMF in control conditions and showed a similar inhibition of miR-142-3p transcription in the presence of actinomycin D in control conditions (one-way ANOVA $p < 0.05$; Figure 6E). This observation suggests that miR-142-3p levels are maintained by a continuous transcription in EAE conditions. MMF likely regulates miR-142-3p at transcriptional level since it was not able to further reduce miR-142-3p in the presence of actinomycin D (Figure 6E). These findings suggest that fumarates have a newly identified direct neuroprotective action on glutamatergic transmission in EAE cerebellum by restoring GLAST/EAAT1 level as a consequence of the reduction of miR-142-3p, with possible effects on miRNA transcription (Figure 7).

DISCUSSION

Previous studies have shown an upregulation of miR-142-3p in MS peripheral blood leukocytes, as well as in autopsy brain tissue, suggesting a role of this molecule in the disease pathogenesis,[41] likely linked to its influence on the immune system.[15–21] Notably, our previous identification in the EAE model and in the CSF of MS patients helped to define miR-142-3p mechanisms of action in the CNS.[28] Here, we consolidated the notion that high levels of miR-142-3p in MS and EAE play an important role in the disease progression. We first observed that the CSF levels of miR-142-3p positively correlated with the PI in a large proportion of MS patients. Accordingly, patients with 'high CSF miR-142-3p' levels consistently showed a worse disease

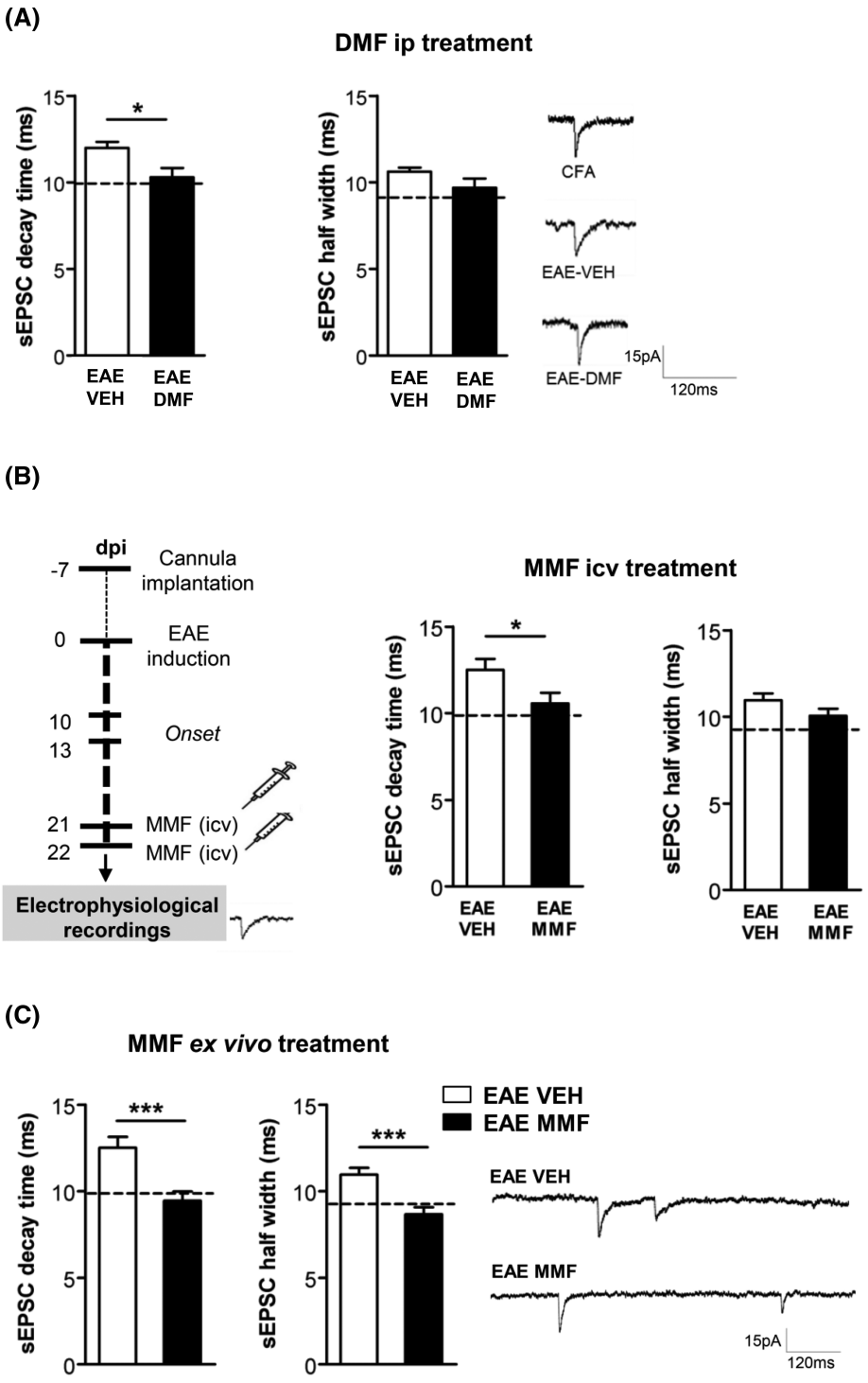

FIGURE 5 Glutamatergic synaptic alterations of EAE cerebellum are mitigated by both DMF (peripheral) and MMF (central and ex-vivo) treatments. (A) Histograms represent the glutamatergic sEPSC kinetic properties (decay time and half-width) recorded from PCs of EAE mice therapeutically treated with DMF (black) or vehicle (white) at peripheral level (daily i.p., 60 mg/kg/day of DMF in 1% DMSO starting on the day of disease onset). The cerebellar sEPSC kinetic properties were in part ameliorated by the DMF treatment (21–28 dpi; EAE-DMF: $n = 15$; EAE-VEH: $n = 10$; unpaired two-tailed t test, decay time $p < 0.05$ and half-width $p > 0.05$). The electrophysiological traces on the right are examples of sEPSC peaks in the different experimental conditions. (B) Histograms represent the glutamatergic sEPSC kinetic properties (decay time and half-width) recorded from PCs of EAE mice treated with monomethyl fumarate (MMF, black) or vehicle (white) delivered at central level (single icv for 2 consecutive days, 0.325 mg/kg/day in PBS-DMSO 0.25%) during the pick of the disease. A central and therapeutic delivery of DMF was sufficient to mitigate cerebellar sEPSC alterations (EAE-VEH: $n = 11$; EAE-MMF: $n = 6$; unpaired two-tailed t test; decay time $p < 0.05$ for and half-width $p > 0.05$). (C) Histograms represent the glutamatergic sEPSC kinetic properties recorded from PCs of EAE cerebellar slices incubated with MMF (2 h, 100 μM in PBS-DMSO 0.001%) or vehicle. MMF was able to completely recover half width and decay time of sEPSC (EAE-VEH: $n = 11$, EAE-MMF: $n = 15$; unpaired two-tailed t test, $p < 0.001$). The electrophysiological traces on the right are examples of sEPSC mean peak in EAE mice. (A–C) Dotted lines represent the mean values obtained in control CFA-untreated mice. Data are presented as mean ± SEM; *$p < 0.05$; ***$p < 0.001$

progression. Furthermore, correlation analysis between miR-142-3p levels and the IL-1 signalling (both Il-1β and IL-1β/IL1-ra) highlighted our previous data on the involvement of the IL-1β-miR-142-3p-GLAST axis in EAE and MS synaptopathy. Of note, previous studies in a CSF-chimeric ex vivo model showed that high levels either of IL-1β/IL-1ra or miR-142-3p were able to induce synaptopathy and/or neurotoxicity in healthy brain slices.[7,35] Accordingly, here we observed that elevated CSF miR-142-3p levels were associated with enhanced response to the iTBS protocol, suggesting increased tendency toward synaptic hyperexcitability in these patients. Although a similar correlation was not observed for IL-1β signalling in this experimental condition, the present results indicate that concomitant high levels of miR-142-3p and IL-1β/IL-1ra circulating in the CSF may promote a worse PI.

Altogether clinical and neurophysiological data suggest that elevated CSF levels of miR-142-3p promote synaptic dysfunction, negatively influencing the disease course of MS. Therefore, selectively targeting miR-142-3p expression may represent an effective

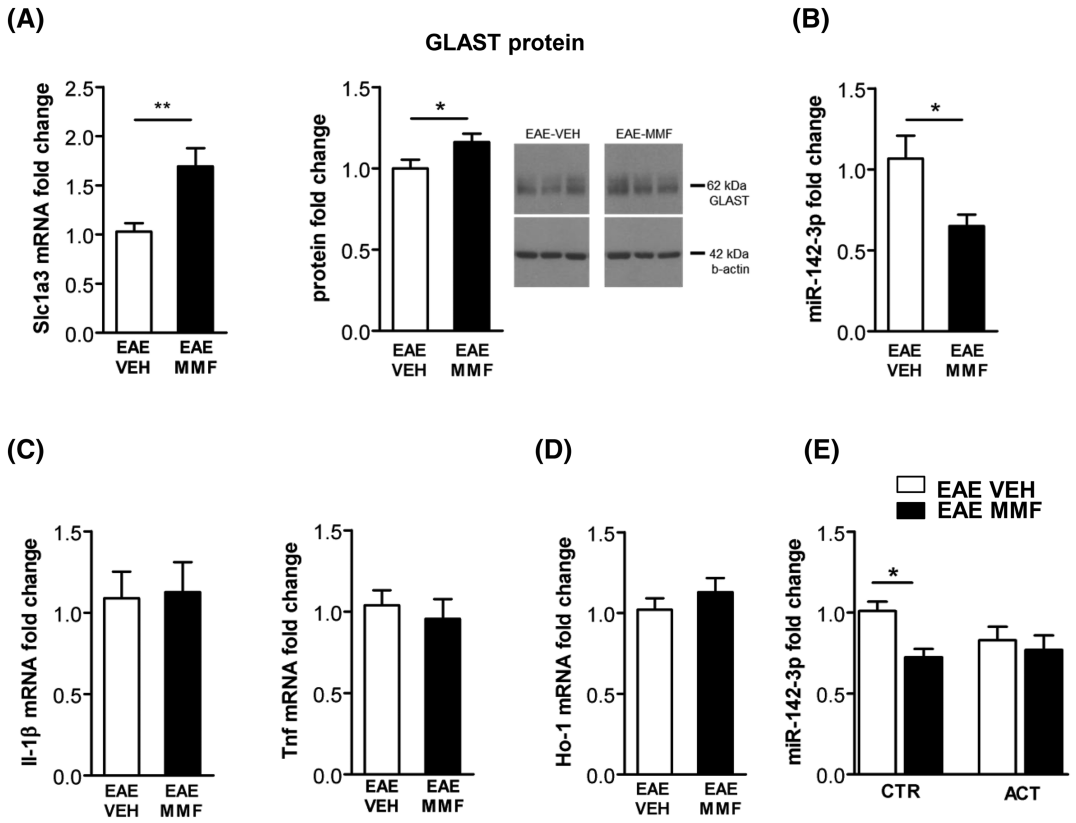

FIGURE 6 MMF disrupts the detrimental regulatory axis IL-1β-miR-142-3p-GLAST to rescue cerebellar glutamatergic transmission. (A) Histograms of Slc1a3 mRNA levels (coding for the glial glutamate transporter GLAST/EAAT1) in EAE cerebellar slices incubated for 2 h with MMF or vehicle (Left, EAE VEH: $n = 9$, EAE MMF: $n = 8$; unpaired two-tailed t test, $p < 0.001$). On the right, representative WB images and quantification of GLAST protein levels (normalised to β-actin) in the same experimental conditions. MMF incubation induces a rescue of GLAST protein in EAE cerebellar slices relatively to EAE untreated slices (Right, EAE-VEH: $n = 12$, EAE-MMF $n = 13$; unpaired two-tailed t test, $p < 0.05$). (B) Histograms showing miR-142-3p levels in EAE cerebellar slices after bath application of MMF (2 h) and vehicle. MMF significantly inhibits miR-142-3p expression (EAE VEH: $n = 9$, EAE MMF: $n = 8$; unpaired two-tailed t test, $p < 0.05$). (C,D) Histograms show no changes of mRNA expression of the proinflammatory cytokines IL-1 β (interleukin-1β; C left) and TNF (tumour necrosis factor; C right), as well as Ho-1 (Heme oxygenase 1; D), a target gene of Nrf2 (nuclear factor (erythroid-derived 2-like) pathway, after 2 h of incubation of EAE cerebellar slices with vehicle or MMF (unpaired two-tailed t test, $p > 0.05$). (E) Histograms shows miR-142-3p levels in EAE cerebellar slices incubated with MMF or vehicle in the presence or not of the transcriptional inhibitor actinomycin D (25 μM; one-way ANOVA Tukey's HSD, $p < 0.05$ EAE-veh vs. EAE MMF and $p > 0.05$ EAE-veh vs. EAE MMF in act condition). (A–E) Data obtained by qPCR were normalised by ΔΔCt calculation to endogenous genes (U6B for miR-142-3p and β-actin for mRNAs). All values are means ± SEM versus EAE-VEH; *$p < 0.05$; **$p < 0.01$

therapeutic strategy to prevent disease progression. We provided an indirect but promising evidence of this latter aspect, by studying the interaction between miR-142-3p and I-line DMT treatments. Accordingly, we found that among patients treated with DMF, lower CSF levels of miR-142-3p at the time of diagnosis were associated with better response to therapy. A similar interaction might occur also for other I-line therapies that have been shown to modulate miR-142-3p at peripheral level, such as glatiramer acetate and INF.[13,14] In the present study, we could not perform this type of evaluation since the number of treated patients for stratification in the two miR-142-3p subgroups, in accordance with their different PI, was not appropriate. In this regard, the present results deserve further attention and investigations since they pave the way for a potential personalised therapeutic approach. Regarding the effect of DMF on miR-142-3p levels, unfortunately the invasiveness of the CSF collecting method impaired a miR-142-3p quantification during the treatment. It could be argued that its detection in serum or plasma could be the most appropriate for monitoring disease progression and response to therapy. However, other studies reported a poor correlation between CSF and plasma findings, suggesting that CSF miRNA profile could provide different information not available in plasma.[42–44]

The anti-inflammatory effects of DMF/MMF have been extensively investigated in clinical and preclinical studies and include a shift toward an anti-inflammatory and more tolerogenic immune profile and a neuroprotective effect against oxidative stress.[45,46] However, its beneficial effects are dependent on multifactorial mechanisms not yet fully known. Here, we observed that EAE miR-142-HE mice were more sensitive to a peripheral and preventive DMF treatment relative to their EAE-WT littermates, showing an improved disease course. This specific effect was associated at peripheral level with a

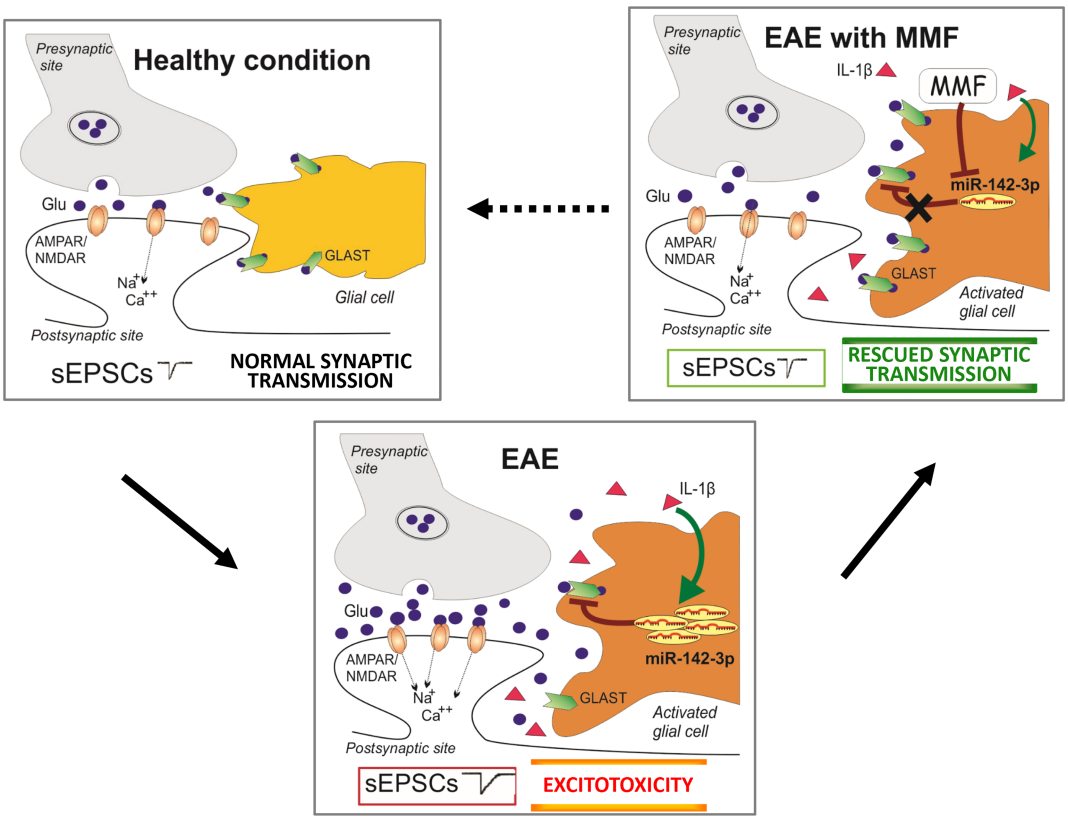

FIGURE 7 Scheme of MMF mechanism of action in counteracting cerebellar synaptopathy. In healthy condition (left), at the level of Purkinje cells in the cerebellum, the clearance of the majority of glutamate released in the synaptic cleft is mainly performed by the glial glutamate transporter GLAST. In EAE condition (bottom), the proinflammatory cytokine IL-1β is responsible of an enhancement of the spontaneous glutamate transmission (sEPSC) by increasing the expression of miR-142-3 which in turn blocks the expression of GLAST (IL-1β-miR-142-3p-GLAST regulatory axis). A long-lasting impairment of glutamate reuptake from the synaptic cleft leads to a persistent cerebellar synaptopathy which causes excitotoxicity. The acute incubation (2 hours) of MMF (right) on EAE cerebellar slices is able to correct the kinetic abnormalities of glutamatergic currents by perturbing the detrimental regulatory axis IL-1β-miR-142-3p-GLAST. Specifically, MMF reduces miR-142-3p expression thus restoring GLAST levels in an IL-1β-independent manner. EAE, experimental autoimmune encephalomyelitis; GLAST, glial glutamate aspartate transporter; Glu, glutamate; IL-1β, interleukin 1 beta; miR-142-3p, microRNA miR-142-3p; MMF, monomethyl fumarate; sEPSCs, spontaneous excitatory post-synaptic currents

modulation of B-cell population and to an increased Treg responsiveness. EAE miR-142 HE mice presented indeed an increase in B cell relative percentage that was suppressed by DMF while Treg cells were more sensitive, relative to Treg cells of EAE-WT mice, to the immune modulation induced by DMF, suggesting an enhanced capability to control autoreactivity. We propose miR-142-HE EAE mice as a good tool to investigate miR-142-depedent EAE pathogenesis and DMF response, likely involving a delicate unbalance of miR-142 expression in several immune cell subtypes, such as B cells[18] and Treg/Teff,[47] as occurs in other inflammatory disease.[48–51] In conclusion, the reduction of miR-142 levels (as in the case of HE mice) may in part be responsible for a more efficient response to DMF, through a modulation of the immune system, in line with evidence showing that elevated levels of miR-142-3p can be detrimental for the pathology itself.

Regarding the interaction between DMF and miR-142-3p at the central level, we explored the impact of DMF therapeutic treatments in WT mice and suggested a mechanistic explanation of its beneficial effect in the CNS pointing to miR-142-3p as a potential new target of this drug. Interestingly, during the characterisation of EAE-miR-142-HE mice, we observed that these mice were protected from EAE synaptopathy, showing a normal glutamatergic transmission even in the presence of an active disease. The same functional recovery was observed in EAE mice treated either at peripheral/therapeutic- or at central/preventive-level with an inhibitor of miR-142-3p,[28] corroborating the notion that treatments that can modulate miR-142-3p might improve at least locally synaptopathic processes. Here, we observed that both therapeutic and central in vivo and ex vivo treatments with fumarates (DMF/MMF) were able to ameliorate the increase in cerebellar glutamatergic transmission in EAE-WT mice. We previously found that a therapeutic and peripheral DMF treatment in EAE mice normalised presynaptic abnormalities of glutamatergic transmission in EAE striatum and that ex vivo MMF modulation of microglial function likely exerted an indirect neuroprotection on striatal synaptic transmission at post-synaptic level.[31,52] It was proposed that MMF had an anti-inflammatory effect of on resident and infiltrating cells in the CNS mediated by the G protein-coupled receptor HCAR2.[52,53] Besides this

pathway, fumarates exert a potent antioxidant effect mainly mediated by activation of the nuclear factor Nrf2, that upregulates several antioxidative pathways (such as the transcription factor Ho-1), and increases glutathione levels.[54] DMF induces Nrf2 in glial cells and neurons in vitro, and in an EAE model. The therapeutic effect of DMF in EAE mice is abolished in Nrf2-knockout mice,[55] even if alternative pathways, independent of Nrf2, have been proposed.[56] Here, we showed that an acute MMF administration was able to ameliorate the excitotoxic damage in EAE cerebellum, proving for the first time the effect of a therapeutic central delivery of MMF on EAE synaptopathy. Mechanistically, we provide evidence that ex vivo acute incubation of MMF on EAE cerebellar slices can reestablish glutamate transmission by restoring the level of GLAST protein, through the reduction of miR-142-3p expression (Figure 7).

The recovery of the miR-142-3p axis mediated by MMF in our experimental condition seems independent of its anti-inflammatory action since the IL-1β mRNA level was not affected as well the inflammatory status of the cerebellum. The unchanged levels of the Ho-1mRNA also indicate that Nrf2 pathway was likely not involved, at least after 2 h of MMF incubation. Accordingly, miR-142 3p was not induced by ex vivo incubation of the Nrf2 activator TAT-14.[40] Altogether these experiments suggest that the classic anti-inflammatory and anti-oxidant pathways are likely not responsible for the acute protective effect of MMF on cerebellar transmission. Here, we point to miR-142-3p as a possible target of MMF through its regulation at the transcriptional level, as suggested by the Actinomycin DMF/MMF experiments. We indeed observed that in the presence of an active transcriptional regulation of miR-142-3p in the EAE cerebellum, MMF was not able to further downregulate miR-142-3p when co-incubated with the transcriptional inhibitor Actinomycin D. Of note, DMF has been shown to inhibit the p90 Ribosomal S6 Kinase 2 (RSK2) and the Mitogen and Stress-activated Kinase (MSK) with implications for transcription.[57]

In conclusion, the huge difficulty of identifying potential biomarkers for MS is due to the multifactorial nature of this complex disease. A scarce knowledge of the several pathophysiological processes and of their interactions as well as the heterogeneity of clinical manifestations have slowed down tailored treatment strategies. Therefore, the research and standardisation of biomarkers linked to specific pathogenic mechanisms is increasingly challenging and special attention should be paid not novel biomarkers in the miRNA family. In the present study, by combining clinical and preclinical studies, we propose miR-142-3p as a potential synaptotoxic and negative prognostic marker of MS disease, and a potential valuable indicator for personalised therapies.

ACKNOWLEDGMENTS

The authors thank Dr. Francesca De Santa from Institute of Cell Biology and Neurobiology (IBCN), National Research Council of Italy (CNR) for her support in qPCR experiments. The authors thank Monica Nencini, Massimo Tolu and Chiara Castelli for helpful technical assistance. The study was supported by a Biogen grant to D.C., FISM grants (Fondazione Italiana Sclerosi Multipla-cod. 2019/S/1 and financed and cofinanced with the '5 per mille' public funding to D.C. and F.R.R. and Fondazione Italiana Sclerosi Multipla-cod. 2016/R/18 and 2018/S/5 to G.Mata.), national funding of the Italian Ministry of University and Research (MIUR-PRIN 2017-cod. 2017K55HLC) to G. Mata and D.C., and of the Italian Ministry of Health (GR-2016-02361163 to A.M.; GR-2016-02362380 to D.F. and F.B.; GR-2016-02363749 to C.P.; GR-2018-12366154 to A.G., C. P and F.B.; RF-2018-12366144 to D.C. and G.M.; Ricerca corrente to IRCCS San Raffaele Pisana to G.M; Ricerca corrente and '5 per mille' public funding to IRCCS Neuromed); Private donation in memory of Chiara Sardi to D.C; F.D.V. was supported by a research fellowship FISM (cod. 2018/B/2) and financed and co-financed with the '5 per mille' public funding.

CONFLICT OF INTEREST

DC is the recipient of an Institutional grant from Biogen. No personal compensation was received. The founding sponsors had no role in the design of the study; in the collection, analyses, or interpretation of data; in the writing of the manuscript, and in the decision to publish the results. F.B. acted as Advisory Board members of Teva and Roche and received honoraria for speaking or consultation fees from Merck Serono, Teva, Biogen Idec, Sanofi, and Novartis and nonfinancial support from Merck Serono, Teva, Biogen Idec, and Sanofi. R.F. received honoraria for serving on scientific advisory boards or as a speaker from Biogen, Novartis, Roche, and Merck and funding for research from Merck. M.S. received research support and consulting fees from Biogen, Merck-Serono, Novartis, Roche, Sanofi, Teva. AU received grants and contracts from FISM, Novartis, Fondazione Cariplo, Italian Ministry of Health; received honoraria or consultation fees from Biogen, Roche, Teva, Merck, Genzyme, Novartis. G. Mata reports grants and/or personal fees from Merck, Novartis, Biogen Idec, and Ibsa. DC is an Advisory Board member of Almirall, Bayer Schering, Biogen, GW Pharmaceuticals, Merck Serono, Novartis, Roche, Sanofi-Genzyme, and Teva and received honoraria for speaking or consultation fees from Almirall, Bayer Schering, Biogen, GW Pharmaceuticals, Merck Serono, Novartis, Roche, Sanofi-Genzyme, and Teva. He is also the principal investigator in clinical trials for Bayer Schering, Biogen, Merck Serono, Mitsubishi, Novartis, Roche, Sanofi-Genzyme, and Teva. His preclinical and clinical research was supported by grants from Bayer Schering, Biogen Idec, Celgene, Merck Serono, Novartis, Roche, Sanofi-Genzyme and Teva. The funders had no role in the design of the study; in the collection, analyses, or interpretation of data; in the writing of the manuscript, or in the decision to publish the results. The other authors declare that they have no competing interests.

ETHICS STATEMENT

This observational prospective study was carried out in compliance with the Declaration of Helsinki principles and was approved by the Institutional Review Board (NCT03217396 recorded in https://clinicaltrials.gov/) of the IRCCS Istituto Neurologico Mediterraneo (INM) Neuromed in Pozzilli (Isernia, Italy). All subjects provided their written informed consent. All details are provided in the Supporting Information.

AUTHOR CONTRIBUTIONS

FDV, AM, DC and GM conceived, designed the research study and wrote the manuscript. AM, DF, FRR, SC, SB and KS conducted, acquired and analyzed electrophysiological data. FDV, AG, SB, LG and VV conducted, acquired and analyzed biochemical and molecular biology data. CP, AC, CF, SB and GMat conducted, acquired and interpreted immune profile analysis. FDV, AM, MSB, GM, LGi, VL, JD and TP analyzed clinical data. MSB, FB, AB and ED collected clinical data. EH provided the transgenic mice and critically contributed to the interpretation of data. RF and AF conducted, acquired and analyzed cytokines profile. AU and MS critically contributed to the interpretation of clinical data. All the authors critically revised the article for important intellectual content and approved the version to be published. FDV and AM contributed equally to this work, as first authors. DC and GM contributed equally to this work, as senior authors.

TRANSPARENT PEER REVIEW

The peer review history for this article is available at https://publons.com/publon/10.1111/nan.12765.

DATA AVAILABILITY STATEMENT

The data that support the findings of this study are available from the corresponding author upon reasonable request.

ORCID

Diego Centonze https://orcid.org/0000-0002-8390-8545
Georgia Mandolesi https://orcid.org/0000-0003-3612-6820

REFERENCES

1. Dendrou CA, Fugger L, Friese MA. Immunopathology of multiple sclerosis. *Nat Rev Immunol*. 2015;15(9):545-558.
2. Reich DS, Lucchinetti CF, Calabresi PA. Multiple sclerosis. *N Engl J Med*. 2018;378(2):169-180.
3. Hou Y, Jia Y, Hou J. Natural course of clinically isolated syndrome: a longitudinal analysis using a Markov model. *Sci Rep*. 2018;8(1):10857.
4. Feuillet L, Reuter F, Audoin B, et al. Early cognitive impairment in patients with clinically isolated syndrome suggestive of multiple sclerosis. *Mult Scler*. 2007;13(1):124-127.
5. De Stefano N, Giorgio A, Battaglini M, et al. Assessing brain atrophy rates in a large population of untreated multiple sclerosis subtypes. *Neurology*. 2010;74(23):1868-1876.
6. Kappos L, Butzkueven H, Wiendl H, et al. Greater sensitivity to multiple sclerosis disability worsening and progression events using a roving versus a fixed reference value in a prospective cohort study. *Mult Scler J*. 2018;24(7):963-973.
7. Mandolesi G, Gentile A, Musella A, et al. Synaptopathy connects inflammation and neurodegeneration in multiple sclerosis. *Nat Rev Neurol*. 2015;11(12):711-724.
8. Li Z, Rana TM. Therapeutic targeting of microRNAs: current status and future challenges. *Nat Rev Drug Discov*. 2014;13(8):622-638.
9. van den Berg MMJ, Krauskopf J, Ramaekers JG, Kleinjans JCS, Prickaerts J, Briedé JJ. Circulating microRNAs as potential biomarkers for psychiatric and neurodegenerative disorders. *Prog Neurobiol*. 2020;185:101732.
10. Huang Q, Xiao B, Ma X, et al. MicroRNAs associated with the pathogenesis of multiple sclerosis [Internet]. *J Neuroimmunol*. 2016;295–296:148-161.
11. Mohammed EM. Environmental influencers, microRNA, and multiple sclerosis. *J Cent Nerv Syst Dis*. 2020;12:1-32.
12. Arruda LCM, Lorenzi JCC, Sousa APA, et al. Autologous hematopoietic SCT normalizes miR-16, -155 and -142-3p expression in multiple sclerosis patients. *Bone Marrow Transplant*. 2015;50(3):380-389.
13. Manna I, Iaccino E, Dattilo V, et al. Exosome-associated miRNA profile as a prognostic tool for therapy response monitoring in multiple sclerosis patients. *FASEB J. Off. Publ. Fed. Am. Soc. Exp. Biol*. 2018;32(8):4241-4246.
14. Waschbisch A, Atiya M, Linker RA, Potapov S, Schwab S, Derfuss T. Glatiramer acetate treatment normalizes deregulated microRNA expression in relapsing remitting multiple sclerosis. *PLoS One*. 2011;6(9):1-5.
15. Gao J, Gu J, Pan X, et al. Blockade of miR-142-3p promotes anti-apoptotic and suppressive function by inducing KDM6A-mediated H3K27me3 demethylation in induced regulatory T cells. *Cell Death Dis*. 2019;10(5):332.
16. Huang B, Zhao J, Lei Z, et al. miR-142-3p restricts cAMP production in CD4+CD25- T cells and CD4+CD25+ TREG cells by targeting AC9 mRNA. *EMBO Rep*. 2009;10(2):180-185.
17. Keller A, Leidinger P, Lange J, et al. Multiple sclerosis: microRNA expression profiles accurately differentiate patients with relapsing-remitting disease from healthy controls. *PLoS One*. 2009;4(10):e7440.
18. Kramer NJ, Wang WL, Reyes EY, et al. Altered lymphopoiesis and immunodeficiency in miR-142 null mice. *Blood*. 2015;125(24):3720-3730.
19. Merkerova M, Belickova M, Bruchova H. Differential expression of microRNAs in hematopoietic cell lineages. *Eur J Haematol*. 2008;81(4):304-310.
20. Mildner A, Chapnik E, Manor O, et al. Mononuclear phagocyte miRNome analysis identifies miR-142 as critical regulator of murine dendritic cell homeostasis. *Blood*. 2013;121(6):1016-1027.
21. Sun Y, Oravecz-Wilson K, Bridges S, et al. miR-142 controls metabolic reprogramming that regulates dendritic cell activation. *J Clin Invest*. 2019;129(5):2029-2042.
22. Gandhi R. miRNA in multiple sclerosis: search for novel biomarkers [Internet]. *Mult. Scler J*. 2015;21(9):1095-1103.
23. Ma X, Zhou J, Zhong Y, et al. Expression, regulation and function of microRNAs in multiple sclerosis. *Int J Med Sci*. 2014;11(8):810-818.
24. Angerstein C, Hecker M, Paap BK, et al. Integration of MicroRNA databases to study MicroRNAs associated with multiple sclerosis. *Mol Neurobiol*. 2012;45(3):520-535.
25. Junker A, Krumbholz M, Eisele S, et al. MicroRNA profiling of multiple sclerosis lesions identifies modulators of the regulatory protein CD47. *Brain*. 2009;132(12):3342-3352.
26. Lescher J, Paap F, Schultz V, et al. MicroRNA regulation in experimental autoimmune encephalomyelitis in mice and marmosets resembles regulation in human multiple sclerosis lesions [Internet]. *J Neuroimmunol*. 2012;246(1–2):27-33.
27. Talebi F, Ghorbani S, Chan WF, et al. MicroRNA-142 regulates inflammation and T cell differentiation in an animal model of multiple sclerosis. *J Neuroinflammation*. 2017;14(1):1-14.
28. Mandolesi G, De Vito F, Musella A, et al. miR-142-3p is a key regulator of IL-1beta-dependent synaptopathy in neuroinflammation. *J Neurosci*. 2017;37(3):546-561.
29. Di Filippo M, Portaccio E, Mancini A, Calabresi P. Multiple sclerosis and cognition: synaptic failure and network dysfunction. *Nat Rev Neurosci*. 2018;19(10):599-609.
30. Geurts JJ, Barkhof F. Grey matter pathology in multiple sclerosis. *Lancet Neurol*. 2008;7(9):841-851.
31. Centonze D, Muzio L, Rossi S, et al. Inflammation triggers synaptic alteration and degeneration in experimental autoimmune encephalomyelitis. *J Neurosci*. 2009;29(11):3442-3452.

32. Gentile A, De Vito F, Fresegna D, et al. Peripheral T cells from multiple sclerosis patients trigger synaptotoxic alterations in central neurons. *Neuropathol Appl Neurobiol*. 2020;46(2):160-170.
33. Mandolesi G, Rizzo FR, Balletta S, et al. The microRNA let-7b-5p is negatively associated with inflammation and disease severity in multiple sclerosis. *Cell*. 2021;10(2):1-21.
34. Mandolesi G, Musella A, Gentile A, et al. Interleukin-1β alters glutamate transmission at purkinje cell synapses in a mouse model of multiple sclerosis. *J Neurosci*. 2013;33(29):12105-12121.
35. Rossi S, Furlan R, De Chiara V, et al. Interleukin-1β causes synaptic hyperexcitability in multiple sclerosis. *Ann Neurol*. 2012;71(1):76-83.
36. Li H, Hu F, Zhang Y, Li K. Comparative efficacy and acceptability of disease-modifying therapies in patients with relapsing–remitting multiple sclerosis: a systematic review and network meta-analysis. *J Neurol*. 2020;267(12):3489-3498.
37. Lucchetta RC, Tonin FS, Borba HHL, et al. Disease-modifying therapies for relapsing-remitting multiple sclerosis: a network meta-analysis. *CNS Drugs*. 2018;32(9):813-826.
38. Scannevin RH, Chollate S, Jung MY, et al. Fumarates promote cytoprotection of central nervous system cells against oxidative stress via the nuclear factor (erythroid-derived 2)-like 2 pathway. *J Pharmacol Exp Ther*. 2012;341(1):274-284.
39. Wierinckx A, Brevé J, Mercier D, Schultzberg M, Drukarch B, Van Dam AM. Detoxication enzyme inducers modify cytokine production in rat mixed glial cells. *J Neuroimmunol*. 2005;166(1–2, 132):132-143.
40. Steel R, Cowan J, Payerne E, O'Connell MA, Searcey M. Anti-inflammatory effect of a cell-penetrating peptide targeting the Nrf2/Keap1 interaction. *ACS Med Chem Lett*. 2012;3(5):407-410.
41. Luo D, Fu J. Identifying characteristic miRNAs-genes and risk pathways of multiple sclerosis based on bioinformatics analysis. *Oncotarget*. 2018;9(4):5287-5300.
42. Bergman P, Piket E, Khademi M, et al. Circulating miR-150 in CSF is a novel candidate biomarker for multiple sclerosis. *Neurol Neuroimmunol Neuroinflamm*. 2016;3(3):e219.
43. Munõz-San Martín M, Reverter G, Robles-Cedeño R, et al. Analysis of miRNA signatures in CSF identifies upregulation of miR-21 and miR-146a/b in patients with multiple sclerosis and active lesions. *J Neuroinflammation*. 2019;16(1):1-10.
44. Raoof R, Jimenez-Mateos EM, Bauer S, et al. Cerebrospinal fluid microRNAs are potential biomarkers of temporal lobe epilepsy and status epilepticus. *Sci Rep*. 2017;7(1):3328.
45. Mills EA, Ogrodnik MA, Plave A, Mao-Draayer Y. Emerging understanding of the mechanism of action for dimethyl fumarate in the treatment of multiple sclerosis. *Front. Neurol.* 2018;9(Jan):1-8.
46. Valencia-Sanchez C, Carter JL. An evaluation of dimethyl fumarate for the treatment of relapsing remitting multiple sclerosis. *Expert Opin Pharmacother*. 2020;00(00):1-7.
47. Anandagoda N, Willis JCD, Hertweck A, et al. MicroRNA-142–mediated repression of phosphodiesterase 3B critically regulates peripheral immune tolerance. *J Clin Invest*. 2019;129(3):1257-1271.
48. Boeschoten RE, Braamse AMJ, Beekman ATF, et al. Journal of the neurological sciences prevalence of depression and anxiety in multiple sclerosis : a systematic review and meta-analysis [Internet]. *J Neurol Sci*. 2017;372:331-341.
49. Dekkema GJ, Bijma T, Jellema PG, et al. Increased miR-142-3p expression might explain reduced regulatory T cell function in granulomatosis with polyangiitis. *Front Immunol*. 2019;10:2170.
50. Ding S, Zhang Q, Luo S, et al. BCL-6 suppresses miR-142-3p/5p expression in SLE CD4+ T cells by modulating histone methylation and acetylation of the miR-142 promoter. *Cell Mol Immunol*. 2020;17(5):474-482.
51. Dolff S, Abdulahad WH, Wilde B. Intrinsic T-cell regulator miR-142-3p/5p—a novel therapeutic target?. *Cell Mol Immunol*. 2021;18(2):508-509.
52. Parodi B, Rossi S, Morando S, et al. Fumarates modulate microglia activation through a novel HCAR2 signaling pathway and rescue synaptic dysregulation in inflamed CNS. *Acta Neuropathol*. 2015;130(2):279-295.
53. Chen H, Assmann JC, Krenz A, et al. Hydroxycarboxylic acid receptor 2 mediates dimethyl fumarate's protective effect in EAE Find the latest version: brief report hydroxycarboxylic acid receptor 2 mediates dimethyl fumarate's protective effect in EAE. *J Clin Invest*. 2014;124(5):2188-2192.
54. Gold R, Linker RA, Stangel M. Fumaric acid and its esters: an emerging treatment for multiple sclerosis with antioxidative mechanism of action. *Clin Immunol*. 2012;142(1):44-48.
55. Linker RA, Lee DH, Ryan S, et al. Fumaric acid esters exert neuroprotective effects in neuroinflammation via activation of the Nrf2 antioxidant pathway. *Brain*. 2011;134(3):678-692.
56. Schulze-Topphoff U, Varrin-Doyer M, Pekarek K, et al. Dimethyl fumarate treatment induces adaptive and innate immune modulation independent of Nrf2. *Proc Natl Acad Sci U S a*. 2016;113(17):4777-4782.
57. Andersen JL, Gesser B, Funder ED, et al. Dimethyl fumarate is an allosteric covalent inhibitor of the p90 ribosomal S6 kinases. *Nat. Commun.* 2018;9(1):4344.

SUPPORTING INFORMATION

Additional supporting information may be found in the online version of the article at the publisher's website.

How to cite this article: De Vito F, Musella A, Fresegna D, et al. MiR-142-3p regulates synaptopathy-driven disease progression in multiple sclerosis. *Neuropathol Appl Neurobiol*. 2022;48(2):e12765. doi:10.1111/nan.12765